New Sustainable Operation Method for a Power Grid without an Energy Storage System: A Case Study of a Hospital in Japan

Yuji Mizuno*‡, Masaharu Tanaka**, Yoshito Tanaka***, Fujio Kurokawa****, Nobumasa Matsui***

*Department of Medical Science, Faculty of Medical Science and Health-Promotion,
Osaka Electro-Communication University, 1130-70 Kiyotaki, Shijonawate-shi, Osaka 575-0063 Japan

**Department of Applied Information Technology, Faculty of Applied Information Technology,
Nagasaki Institute of Applied Science, 536 Aba-machi, Nagasaki-shi, Nagasaki, 851-0193 Japan

***Department of Engineering, Faculty of Engineering,
Nagasaki Institute of Applied Science, 536 Aba-machi, Nagasaki-shi, Nagasaki, 851-0193 Japan

****Institute for Innovative Science and Technology,
Nagasaki Institute of Applied Science, 3-1 Shuku-machi, Nagasaki-shi, Nagasaki, 851-0121 Japan

(y-mizuno@osakac.ac.jp, tanaka_masaharu@nias.ac.jp, tanaka_yoshito@nias.ac.jp, kurokawa_fujio@nias.ac.jp, matsui_nobumasa@nias.ac.jp)

‡Corresponding Author; Yuji Mizuno, 1130-70 Kiyotaki, Shijonawate-shi, Osaka 575-0063 Japan, Tel: +81 72 876 3317,
y-mizuno@osakac.ac.jp

Received: 13.07.2022 Accepted:21.08.2022

Abstract- This paper presents a new sustainable operation method for running the power system of a disaster base hospital without the use of an energy storage device. There is a diesel generator for islanded operation in the hospitals in the event of a disaster, but it keeps emptying due to the issue that the fuel stored in the tank deteriorates. In consequence, diesel generators fail to start up and medical services cannot be kept. To prevent fuel deterioration, it is deemed necessary to refuel the tank with occasional use of fuel. Even in hospitals, installing backup power systems like photovoltaics is a common way to reduce energy use. In such hospitals, there is a demand to combine diesel generators and photovoltaics to respond a demand side response. Since it is challenging to operate a complicated system of diesel generators and photovoltaics, it is necessary to install more energy storage system. But several hospitals do not want to install it because energy storage system is so pricey. This paper proposes a method that can correspond demand side response as a virtual power plant in a power grid without an energy storage system to improve the operational issues of a complex combination of diesel generators and photovoltaics. It requires a load prediction first. The prediction method is the load one step ahead prediction and providing the optimized output distribution and rate setting to the diesel generators, stable operation is possible without energy storage system. The proposed method is evaluated by employing a simulation model using the measured photovoltaics output and the actual load at a hospital. As a result, it shows that it can correspond a demand side response of ± 10 % in the season when the load is low at the hospital with a contract demand 980 kW with 20 % of a photovoltaics. Furthermore, it is clarified that it can correspond a demand side response of ± 25 % in the season during peak load seasons.

Keywords Hospital, virtual power plant (VPP), diesel generator (DG), photovoltaic (PV), demand side response (DR), predicted load, machine learning (ML).

1. Introduction

Japan has seen numerous natural disasters, including Typhoon No. 15 in September 2019 and Typhoon No. 19 in October 2019 [1]. Following the Kumamoto earthquake in April 2016 [2], a significant power outage persisted for roughly a week. Also, the eastern Hokkaido Iburi earthquake in September 2018 forced an emergency stop of the Tomato-Atsuma thermal power plant, leaving 2.95 million homes with blackout [3],[4]. In response to such disasters and power system accidents, hospitals are equipped with diesel generators (DGs) that are based on Japanese Industrial Standards (JIS) [5]. DGs also encourage energy conservation by using distributed energy, which actively utilizes renewable energy. The standard operating time is 72 h at disaster base hospitals, and there has been a gap between recent long-term disaster recoveries and the actual power reserves. Diesel generators use fossil fuels, and one issue is how to ensure that the required fuel is available during a disaster when the time of use is unclear. Fuel that has degraded beyond usage is discarded, which can have negative environmental effects [6]. Therefore, the fuel tanks of small- and medium-sized hospitals may be empty even though there is a DG system. In consequence, DGs fail to start up and medical services cannot continue. It is vital to occasionally refuel the tank with fuel to avoid fuel degradation. Installation of backup power system, such as photovoltaics (PV), is becoming popular measures against energy saving even in hospitals. Since it is challenging to operate a complicated system of DGs and PV, it is necessary to install more energy storage system (ESS). But several hospitals do not want to install it because ESS is so pricey.

In the previous studies, assuming the combined use of DGs and PV in a large hospital, an energy management system (EMS) that can power in long-term island mode and continue medical services has been proposed. In a hospital with a single 1,000-kVA DG, assuming islanded operation in the event of a disaster, the conventional DG is miniaturized as a distributed power source, and renewable energy is taken into account during the installation planning. It also suggested an optimization method that is decentralized and minimized fuel consumption by operating multiple DGs. There are two proposed optimization method: one is linear programming [7],[8] the other is genetic algorithm [9].

Assuming the combined use of DGs and PV, the electric power balance during islanding have been evaluated, from the historical total load in a hospital. In these studies, it examined the load prediction method that is learned by a machine learning from the actual total load in the hospital and the meteorological data published by the Japan Meteorological Agency and combined with the EMS [10]. In addition, experiments are conducted using a power emulator, that the proposed EMS can deliver a steady power supply even throughout a week of islanded operation [11].

As per further investigation, it was found that there is a new issue with respect to the deterioration of fuel in the tank [6]. Based on the results of previous studies, the next study proposed to deal with the power system of the hospital as a virtual power plant (VPP) [12]. A VPP can be defined as a cluster of dispersed generating units, flexible loads, and storage systems that are grouped to operate as a single entity. The generating units in a VPP can employ both fossil and renewable energy sources [13]. A VPP can be realized by utilizing advanced energy management technology to integrate renewable energy that is distributed energy resources such as storage batteries, and a demand side response (DR), which is an advanced demand management method.

The reference [12] proposes to keep the net demand constant by using output of PV and DGs. However, it has not been able to respond to a rise and reduction of DR. Moreover, when the power demand of the overall power system is low and the output of photovoltaic power generation is high, the aggregator requests that the output of photovoltaic power generation be suppressed.

Therefore, this paper proposes a method that can correspond a DR as a VPP in a power grid without an ESS in order to address the operational issues of a complicated combination of DGs and PV. It requires a load prediction first. The prediction method is the load one step ahead prediction and providing the optimized output distribution and rate setting to the DGs, stable operation is possible without ESS. The proposed method is evaluated by employing a simulation model using the measured PV output and the actual load at a hospital.

The contribution of the paper, can be outlined as follows:

1) In terms of generator fuel, it is possible to effectively use the fuel that would be discarded due to deterioration of long-term storage.
2) It is possible to decrease the trouble that DG does not start up due to the disaster.
3) A hospital as VPP can get a reward by operating DR according to the request of an aggregator. The reward may cover some of the cost of the fuel.
4) It is possible to deal with DR without limiting the output of self-consumed PV. In other words, it can contribute keep the utility power grid stable.

The rest of this paper is organized as follows. Section II introduces a hospital grid integrated with PVs as a VPP, and the proposed model and control of a VPP are described in Section III. Section IV explains the model validation is provided. Finally, Section V provides the conclusions and outlook.

2. Hospital Grid Integrated with PVs as a Virtual Power Plant

Recently, there has been a growing number of hospitals installing a PV system on energy saving or environmental issues. The reference [13] provides guidance for redesigning existing hospitals based on a concept of microgrids by installing PV systems. It also reports that improving the power grid will improve the quality of medical services.

Figure 1 shows a utility grid and an emergency power system with coupled DGs as the diesel generator and a PV system.

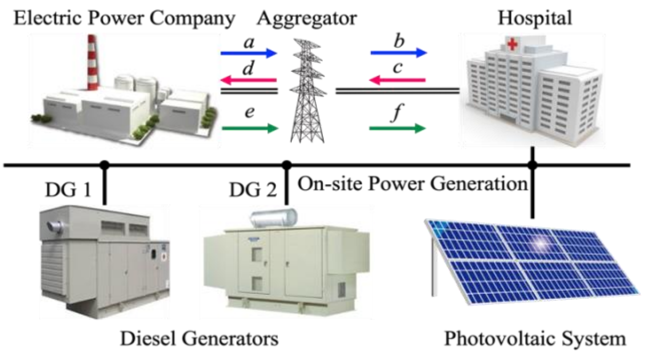

Fig. 1. Configuration for a hospital grid as a VPP.

The area where PV can be installed on the hospital is exactly 20 % of the contract demand in this study, which is 980 kW. The hospital load, DGs and PVs are connected to a grid of on-site power generation. Depending on the DR signal, the DGs start, and the supply power is managed by the EMS for optimal operation with the minimization of fuel consumption.

Aggregator controls a trading between the supply and demand of power. The trading procedure is as follows from *a* to *f*.

a. Aggregator receives a DR request from the electric power company.

b. Aggregator requests to the customer.

c. Aggregator aggregates the amount of demand from consumers.

d. Aggregator provides demand to the electric power company.

e. Aggregator receives a reward from the electric power company.

f. Aggregator pays the reward to the customer.

3. Proposed Model and Control of a Virtual Power Plant

Even in the case of VPP compatibility with the power system, the system model is evaluated under the same conditions, considering the shift to islanded operation mode. However, evaluating the responsibility of DGs in an ESS is beyond the scope of this study.

In the following Subsection 3.1 explains a system model. An operation method for VPP is describes in Subsection 3.2. Subsection 3.3 explains the predicted hospital load model. Optimum energy scheduling method of DGs using linear programming for the minimization of fuel consumption is provided in Subsection 3.4. Subsection 3.5 is explanation of DGs and control model and an operation limit of DGs.

3.1. System Model

Figure 2 shows the block diagram of a distributed power system model that consists of DGs and a PV system in the hospital. The system model takes the weather, PV output, and hospital load as inputs. A machine learning (ML) algorithm then predicts the hospital load using the one-step-ahead prediction load as the training goal data. PV output scales conversion that is performed using actual measurement values, and the data is given to a simulation model to evaluate the effectiveness of the proposed method. So, since the measured values are used, predicting a PV output is not required.

The output target value of the DGs is obtained by subtracting the PV output and the net demand target values from a load of the one-step-ahead prediction. For the output target value, an optimization method utilizing linear programming is used to determine the distribution of the generator output that minimizes the overall fuel consumption; then, the DG output target and rate of change are determined for each of the DGs. The system model is characterized by an algorithm that provides the rate of change to the generator using the load predicted by an ML, one-step-ahead prediction. Additionally, the system model can support both a connected mode on the utility grid and an islanded operation mode.

3.2. Operation Method for Virtual Power Plant

Figure 3 shows a scheme of the proposed operation method for a VPP in a hospital. Effective power [kW] is on the vertical axis, while time [hour] is on the horizontal axis. The green area represents the PV power generation, and the red area represents the power generated by DGs. The net demand is shown by the cyan region.

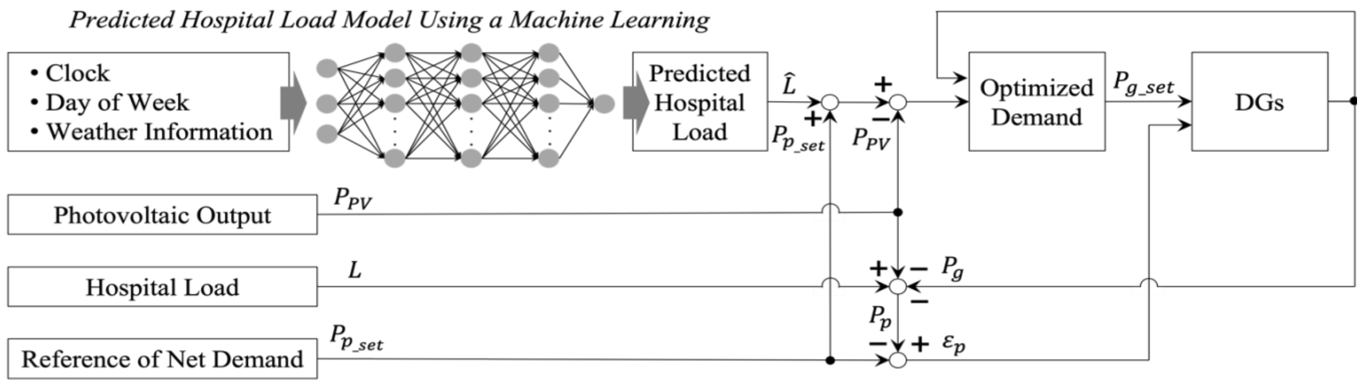

Fig. 2. Block diagram of the proposed method for a VPP.

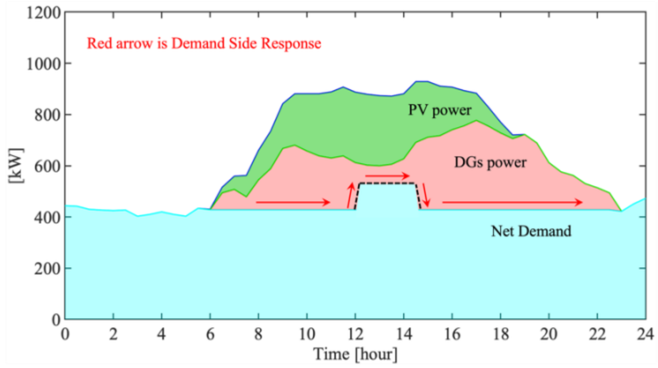

Fig. 3. Scheme of the proposed method for a VPP.

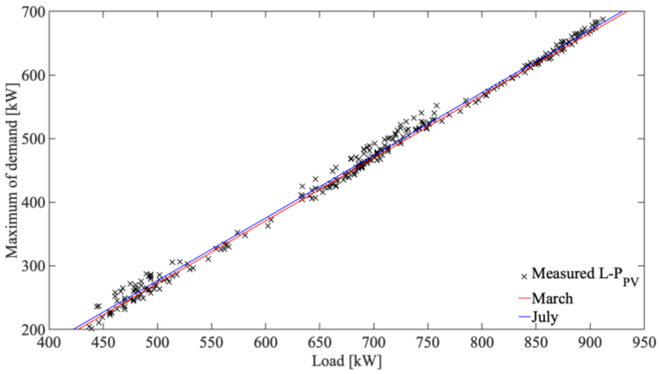

Fig. 4. Maximum of demand.

The proposed operation method for a VPP in a large hospital is as follows, assuming that the demand increases depending on increasing the PV output during the daytime:

(Step 1) The DGs start in control with minimized fuel consumption.

(Step 2) No control restrictions on the PV output in the large hospital.

(Step 3) Net demand controls depend on the demand side response target value.

The papers [14]-[16] report that a DR contributes to the stability of the power system. The proposed method also contributes to stability of the utility power grid.

Figure 4 shows the maximum demand using DGs in March and July. Maximum demand [kW] is on the vertical axis, while hospital load [kW] is on the horizontal axis. The figure makes from multiple regression model in Eq. (1), where L is the measured hospital load, P_{PV} is the measured PV output, through k_1 and k_3 are coefficient of multiple regression, as shown in Table 1.

$$P_{p\_set\_max} = k_1 L + k_2 P_{PV} + k_3 \tag{1}$$

Table 1. Regression parameters

k_1	k_2	k_3
−224.1452	1.0987	0.9859

3.3. Predicted Hospital Load Model

The paper [17] proposed the optimum operation schedule for distributed power sources using DGs, PV, ESS, and so on. However, the report appears to have a practical issue because overshoots and undershoots occur because the rate of change of the power source is not taken into account during the operation. Therefore, it estimates a load of one-step-ahead prediction to consider the rate of change in load in this paper.

Actual load time series, actual load time, actual load day of the week, actual road weather information vector one step before (past), and actual load time series vector are all employed in the training target. In particular, it is easy to handle using the actual load data in the input layer without feeding it back to the hidden layer. An ML configuration diagram is shown in Fig. 2. Following learning, the load at time n is predicted using the day of the week at time n, the weather information data, i.e., the temperature at time $(n-1)$, and the load at time $(n-1)$. Generators can be stabilized by reducing the overshoot or undershoot because the DG controller can make a change in the rate of the DG output from the current load to the predicted load.

In this model, by understanding n and one-step-ahead prediction $(n+1)$, it is possible to give the next output target value and change the rate-setting value from EMS to DG. The data sampling time is set to 10 minutes because the meteorological data of the Japan Meteorological Agency (JMA) is published every 10 minutes.

In Eq. (2), u is the input sum of each neuron, x is the input value, w is the weight factor, θ is the bias, and M is the number of constituent neurons in each layer [18]-[20]. In Eq. (3), $f(u)$ is the activation function and z is the output of each element.

$$u = \theta + \sum_{k=1}^{M} w_k x_k \tag{2}$$

$$z = f(u) \tag{3}$$

Equation (4) shows the activation of the output layer as an identity function. $\hat{L}$ is the predicted hospital load by an ML.

$$\hat{L} = f(u) = u \tag{4}$$

The training error ΔE is evaluated using the mean squared normalized error performance function shown in Eq. (5), where L is measured hospital load and n is a number of data.

$$\Delta E = \frac{1}{n}\sum_{k=1}^{n}\left(L(t) - \hat{L}(t)\right)^2 \tag{5}$$

MATLAB provides a solver for an ML. The parameter “trainbr” of MATLAB can train any network as long as the weighting function, net input function, and transfer function have derivatives. The linear combination of error and weight squares is minimized through Bayesian regularization. After training, it changes the linear combination to enhance the network’s generalization quality [18]. Also, “trainlm” is Levenberg-Marquardt optimization of a network training function that updates weight and bias values, and an improved version of it has also been proposed [19],[20].

Figure 5 shows the flow chart in an ML for predicting the hospital load. The first stage includes the dataset of clock, day of week, weather information and hospital load are given at the first step. The correlation of load prediction using weather information data has also been reported in past papers using an ML [21],[22]. Additionally, changes in weather, holidays,

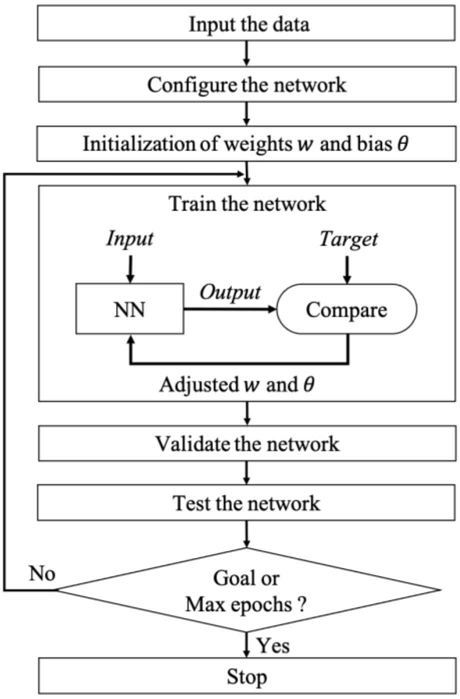

Fig. 5. Flow chart of a machine learning predicting hospital load.

weekends, and other factors can affect power use, with the temperature being cited as the weather information data with the greatest impact [23]. So, the load prediction method is used weather information as an input of an ML in this study. Weather information data can be obtained from the JMA in Japan. The database of JMA provides air temperature, precipitation, wind speed, and wind direction in the area where is locate of the hospital.

Next step, the dataset partition is defined for training, validation, and testing, the solver is selected. Also, the data partitioning should be defined. The data partitioning methods are 70 % of the entire Dataset for training, 15 % of the entire Dataset for validation, and 15 % of the entire Dataset for testing in this study.

In the third step, the initialization of weights and bias is executed. The weights and biases are tweaked to optimize the network performance in network training of the fourth step. The network can adjust weights by comparison until an ML output matches the target. The training dataset determines the ideal weights and biases. The validation dataset determines an algorithmic stopping point or the ideal number of concealed units.

The last phase uses the network; a portion of the gathered data is randomly selected and sent to the network for testing. The training finishes either reaching a maximum number of epochs or performance goal is met.

3.4. Optimization for Minimization of Fuel Consumption

An optimized demand is made to use linear programming for the DGs to minimize their fuel consumption [7],[8]. Based on the manufacturers' specifications for the DGs, the least squares approximation is used to fit the fuel characteristics with the linear equation in Eq. (6).

In Eq. (6), W_{gi} is a rough function representing the relationship between the fuel consumption and generator output when two DGs are employed. The parameters a_i and b_i are characteristics of the DGs, and P_{gi} is the generator output (in kW), where i is the operation number of the DG.

$$W_{gi} - a_i P_{gi} = b_i \tag{6}$$

The reference to the generator P_{g_set} is subtracting $\bar{P}_{PV}$ from $\hat{L}$ as the predicted load. Meanwhile, P_{p_set} is given by the function generator as a demand, where the parameter m is 2 in Eq. (7).

$$P_{g\_set} = \sum_i^m P_{gi\_set} = \hat{L} - \bar{P}_{PV} - P_{p\_set} \tag{7}$$

The equation condition of the linear programming is expressed by Eq. (8) as follows:

$$A_{eq} X = b_{eq} \tag{8}$$

Because this paper uses two generators, A_{eq}, b_{eq}, and X can be given as follows:

$$A_{eq} = \begin{bmatrix} 1 & 0 & -a_1 & 0 \\ 0 & 1 & 0 & -a_2 \\ 0 & 0 & 1 & 1 \\ 0 & 0 & 0 & 0 \end{bmatrix} \tag{9}$$

$$b_{eq} = \begin{bmatrix} b_1 \\ b_2 \\ \hat{L} - \bar{P}_{PV} \\ 0 \end{bmatrix} \tag{10}$$

$$X = \begin{bmatrix} W_{g1} \\ W_{g2} \\ P_{g1\_set} \\ P_{g2\_set} \end{bmatrix} \tag{11}$$

The following inequality conditions are utilized in the linear programming, and the generator's operating range is between 5 % and the rated load. The constraints of inequality for the output powers of the DGs are shown in Eq. (12), where P_{i_R} is the effective power with a power factor of 0.8 and the minimum output is 5 % of the rated value.

$$0.05 \cdot P_{gi_R} \leqq P_{gi\_set} \leqq P_{gi_R} \tag{12}$$

Equation (13) shows the object function for linear programming that identifies the generator output based on the aforementioned criteria that consume the least fuel when two DGs are used [24]. Then, parameter m is given by a constant as 2.

$$\min_{P_{gi}} f = \sum_{i=1}^m W_{gi} \tag{13}$$

The output of a linear programming iterative calculation retains the prior value if there is no numerical solution.

3.5. Diesel Generators and Control Model

Figure 6 shows the DG model in Fig. 2. The generator control model controls the output of the generator model according to the generator output target. RS is a rate setter, C is a controller of DG, and DG is a diesel generator, and the index is several units, where the parameter m is 2.

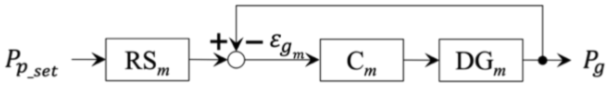

Fig. 6. A diesel generator model in Fig.2.

The model consists of a fuel model, gas turbine model, and generator model [25]. The controller model has the two functions of load control and a proportional control of net demand.

In Fig. 2, the net demand P_p from the utility grid is calculated by subtracting the currently measured load from the DG output and PV output, as shown in Eq. (14). However, there are operational limitations under the circumstances depicted in Eq. (15), where P_{g_min} is the minimum load of the generator.

$$P_p = L - \sum P_g - P_{PV} \tag{14}$$

$$P_{p\_set} < L - P_{PV} - \sum P_{g\_min} \cong P_{p\_set\_max} \tag{15}$$

In addition, ε_g is an error in subtracting P_{g_set} from P_g. P_{g_set} is a reference to the generator output. Finally, ε_p is an error of subtracting a P_{p_set} from P_p, as shown in Eqs. (17) and (18). In Eq. (16), the PI controller is a base controller, so the error ε_g uses the PV output.

However, as the deviation of net demand must be instantly eliminated, the error ε_p for the proportional control directly employs the measured value of the PV production.

$$u_g = K_{PB}\left(\varepsilon_g(t) + K_I\int_0^t \varepsilon_g(\tau)d\tau\right) + K_P\varepsilon_p \tag{16}$$

Here,

$$\varepsilon_g = P_{g\_set} - P_g \tag{17}$$

$$\varepsilon_p = P_{p\_set} - P_p \tag{18}$$

The fuel model of the DGs is shown in Eq. (19). It is a straightforward first-order lag scheme, where W_i is the fuel flow rate, i is the number of the DG, and u_{gi} is the fuel output command of the DG as the manipulated variable. Also, T_1 is a time constant. Here, T_1 is 0.4 s based on the characteristics of the actual machine.

The generator model is shown in Eq. (20). It is a straightforward first-order lag scheme like the fuel model. Here, P_{gi} is the output of DG, i is the number of the DG, W_i is the fuel flow rate, T_2 is a time constant, s is the Laplace operator, and W_i and P_{gi} are normalized. Here, T_2 is 0.2 s based on the characteristics of the actual machine.

$$W_i(s) = \frac{1}{1+T_1 s}u_{gi}(s) \tag{19}$$

$$P_{gi}(s) = \frac{1}{1+T_2 s}W_i(s) \tag{20}$$

The present measured load is subtracted from the expected load of an ML, and the predicted load period is divided by the time interval of the prediction process to get the following equation. Through Eq. (21) and Eq. (23), R_{gi} is given as the rate setter for the generator controller.

$$\Delta t = t(n+1) - t(n) \tag{21}$$

$$R_{gi} = \frac{\hat{P}_{gi}(n+1) - P_{gi}(n)}{\Delta t} \tag{22}$$

$$\left|R_{g_i}\right| \le 0.05 \cdot P_{gi_R} \tag{23}$$

4. Consideration of the Demand Side Response

Even in the case of VPP compatibility with the power system, the system model is evaluated under the same conditions, considering the shift to islanded operation mode. However, evaluating the responsibility of DGs in an ESS is beyond the scope of this study.

According to a statement made by the electric power company that controls the area of hospital, they have demanded an output cap from PV generation businesses in the same area for 206 days for three years. Research on DR in Japan is developing, and the PV output limit will be shifted to DR as a policy of the Agency for Natural Resources and Energy [26].

The output of the PV experimental equipment in March and July, when the output limit was required, will be used in this instance to verify the proposed method. Nearly all the large hospitals have DGs for disasters, but as was already indicated, handling fuel remains to be a major issue. Therefore, in a power system that also uses a PV system, modeling to examine the DR in combination with an DG is described in Section IV. This section will go over how to control of the DR using the models and simulation results.

4.1. Load Prediction

The model by the trained ML is validated in a comparison of the actual load and model load. The fitting results are evaluated by Eqs. (24) and (25), where $\hat{L}$ is the predicted hospital load by an ML, L is the measured hospital load, and n is a number of data.

The root mean squared error (RMSE) and the mean absolute error (MAE) is the indicators to measure the goodness of the numerical prediction model. In addition, when a good model is built, the model accurately captures the fundamental properties of the data, and only the noise that deviates from the normal distribution is regarded as an error. In such cases, RMSE/MAE ratio in the analysis results is close to 1.253 [27].

$$RMSE = \sqrt{\frac{1}{n}\sum_{i=1}^{n}\left(\hat{L} - L\right)^2} \tag{24}$$

$$MAE = \frac{1}{n}\sum_{i=1}^{n}\left|\hat{L} - L\right| \tag{25}$$

Figure 7 shows the results for one week in March and July. The vertical axis is the load power [kW], whereas the horizontal axis is time [hour]. The solid blue line represents an actual hospital load, and the dotted red line represents the predicted load.

Both load patterns share similar characteristics; before 6:00, there is an almost continuous low load, which increases gradually after 6:00 due to preparation for breakfast. After 8:00, the daytime power consumption during the outpatient services time indicates a broad peak. The maximum load denotes 701 kW in March and 929 kW in July, which is the maximum. According to the results of a hospital load survey, the number of outpatients is easily affected by the weather information, and an ML algorithm is employed to take advantage of this causal relationship to increase the accuracy of estimating the overall load of a large hospital.

As a result, in case of the input signal is only the air temperature, the hidden layer is three with thirty neurons, respectively, and one output layer, it is confirmed that the RMSE/MAE between the predicted load value obtained by using 'trainbr'. In case of the input signal is merely the air temperature, an ML establishes by the hidden layer of three with thirty neurons, respectively, and one output layer. It is confirmed that higher performance is obtained using solver of 'trainbr' as an ML. The results are evaluated by using the RMSE/MAE ratio between the predicted load value and the actual load. The daily RMSE/MAE ratio shows between 1.281 and 1.423 in March. It confirms that the daily RMSE/MAE denotes between 1.342 and 1.574 in July. The error in March is calculated using RMSE, it ranges from 2.0 kW to 2.8 kW. There is a 2.2 kW to 3.6 kW inaccuracy in July. It is clarified that the error is within 0.37 % of contract power 980 kW at rated.

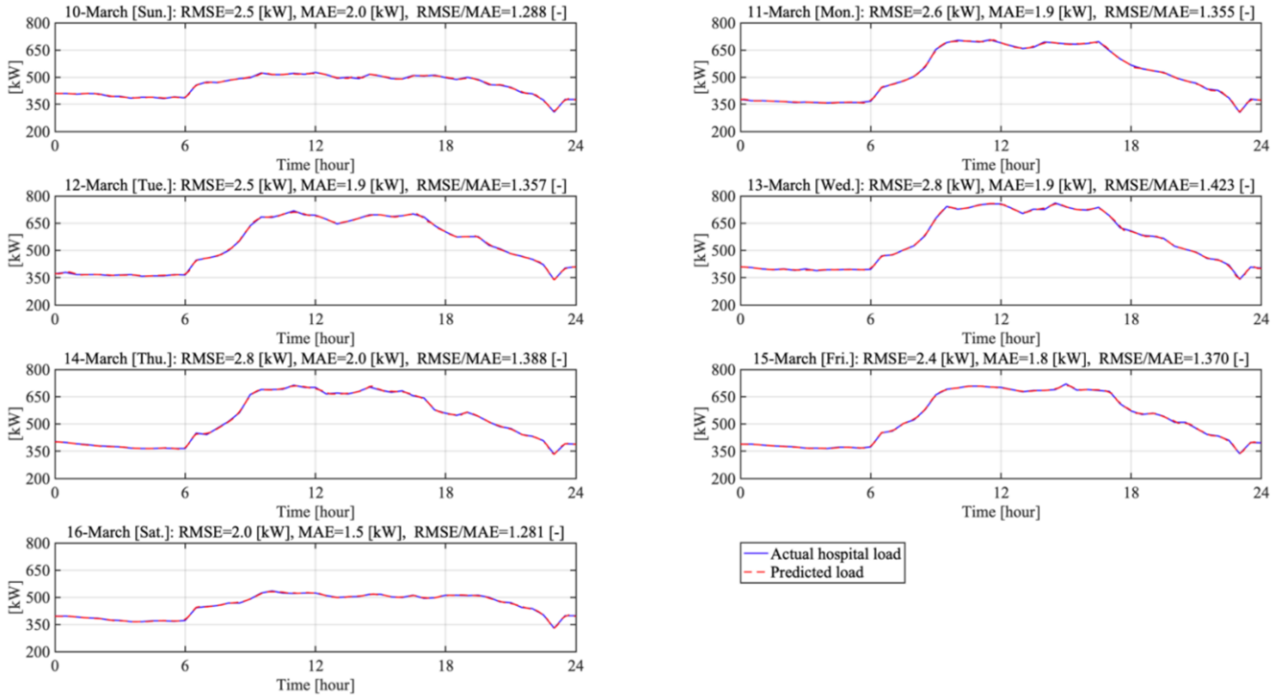

(a) Results of case for a week in March.

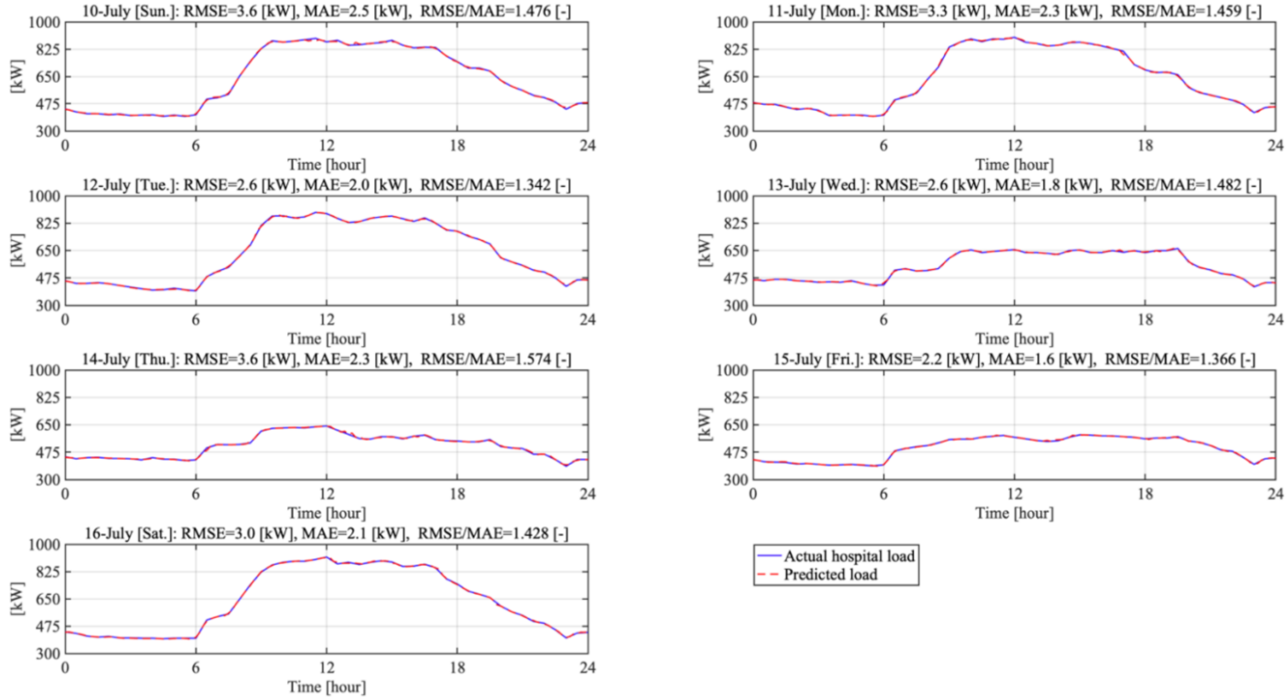

(b) Results of case for a week in July.

Fig. 7. Comparison between the predicted load and actual hospital load.

4.2. Rate of Change of Hospital Load and PV Output

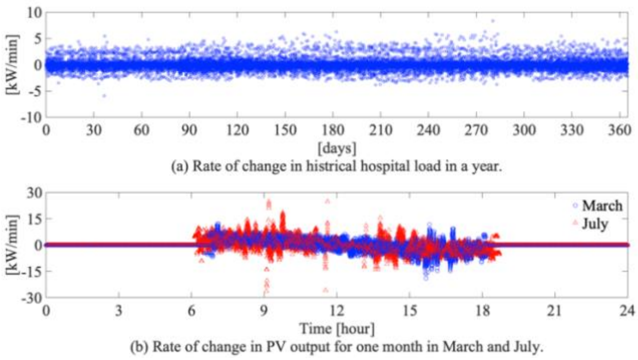

Fig. 8. Rate of change of hospital load and PV output.

In the paper [28], the lamp speed limit of a DG is changed from 4.5 % to 6.2 % in order to observe the effects of the DG. Hence, the output change rate is up to 5 % of the rated output in this paper.

Figure 8 shows a rate of change of hospital load and PV output. The vertical axis is rate power [kW/min], the horizontal axis is days in a year [days] in the upper figure (a), whereas in the lower figure (b) is time in a day [hour]. It is shown that the rate of change in hospital load is between −5.9 and +8.4 kW/min, and the rate of change in PV output in Fig. 8 is between −26.4 and +25.0 kW/min. Given that DGs can adjust their output at a maximum rate of 40 kW/min (5%/min), it is obvious that the rate of change of load and PV is within this range.

4.3. Case Study

4.3.1. Scheduling for demand side response control

In two case studies, the actual load patterns data of a large hospital and the actual performance data of its DGs will be used to demonstrate the effectiveness of the hospital grid configuration and operation method for one day operation of a VPP. The model validation is performed using the pattern of PV power generation in fine weather because it is expected that output suppression of solar power generation will be issued, under the large hospital load in Fig. 7.

The timetable for demand control is shown in Table 2 as a case study. According to the demand rise schedule, the net demand set value increases from 350 to 450 kW between 11:00 and 11:30; it will then remain constant between 11:30 and 13:00 and then decrease to 350 kW between 13:00 and 13:30. In the demand reduction schedule, the net demand set value expected to decreases between 11:00 and 11:30, stays constant between 11:30 and 13:00, and increases between 13:00 and 13:30. Case Study I is analyzed using the measured hospital load in March, the measured hospital load in July is used in Case Study II.

In two case studies, the optimum energy scheduling using linear programming to minimize the fuel consumption using two different generators are selected. These generators have a combination of the same type 500-kVA and 250-kVA and 750-kVA.

Table 2. Scheduling for demand side response control

Demand side response (schedule)	11:00-11:30	11:30-13:00	13:00-13:30
Power in demand rise	↗	→	↘
Power in demand reduction	↘	→	↗

4.3.2. Simulation results for demand side response

Figures 9 shows the simulation results as a Case Study I using the system model of Fig. 2. This case uses the measured load in March of Fig. 7 (a) and the measured PV output data.

In all of the graphs, the vertical axis is power [kW], and the horizontal axis is time, from 0 to 24 [hour]. There are four cases from (a) to (d) in Case Study I. The top and bottom two figures in the first row from the left are the graphs when two 500-kVA generators are used and the DR is raised, as shown in Fig. 9 (a). The two figures in the second row from the left in Fig. 9 (b) are the graphs when two 500-kVA generators are used, and the DR is reduced. In Fig. 9 (c) of the third row from the left are the graphs when the combination 250-kVA and 750-kVA generators are used and the DR is raised, and Fig. 9 (d) of the first row from the right uses the combination of 250-kVA and 750-kVA generators and the DR is reduced.

In the four figures at the top of Fig. 9, the solid blue line shows the hospital load on weekdays in March, the dotted red line represents the predicted load, the solid green line indicates the data obtained by subtracting the amount of PV power generation from the load, and the solid cyan line is the net demand. In the four figures at the bottom of Fig. 9, the solid blue line represents the output of DG 1, whereas the solid red line is the output of DG 2.

The two generators operate from 5 % to 100 % of their respective generating capacities with a maximum rate of change that is limited to 5 % of the rated output per minute. For each generator, an output target value is provided by an optimization algorithm that minimizes the fuel consumption.

Focusing on the DR operation period from 11:30 to 13:30, which is shown by the net demand in light blue, as a result of verification of the change from 350 by ± 99.5 kW based on Eq. (1), the combination of the same type of 500-kVA generator shows that one generator.

According to the optimization for minimization of fuel consumption of Subsection 3.4 in Section III, for the combination of 250-kVA and 750-kVA, the small 250-kVA generator follows the load and when the output of the small generator is deemed insufficient, whereas the large 750-kVA generator is in backup operation. Also, in the case of a DR rise, as shown by Eq. (15), it can be seen that the allowable limit of operation is when the outputs of the two generators reach the minimum.

Figures 10 is as in Fig. 9, but for the results of Case Study II that uses the measured hospital load in July shown in Fig. 7 (b). There are four cases from (a) to (d) in Case Study II. Focusing on the DR operation period as in Fig 10, it can verify the variation from 400 by ± 251 kW based on Eq (1).

For the combination of 250-kVA and 750-kVA, the optimization method and parameters are the same as Case Study I, however, the large 750-kVA generator follows the load. The small 250-kVA generator is in full load operation because the load is higher than Case Study I. Also, in the case of a DR rise, as shown by Eq. (15), it can be seen that the permitted limit of operation is when the outputs of the two generators reach the minimum.

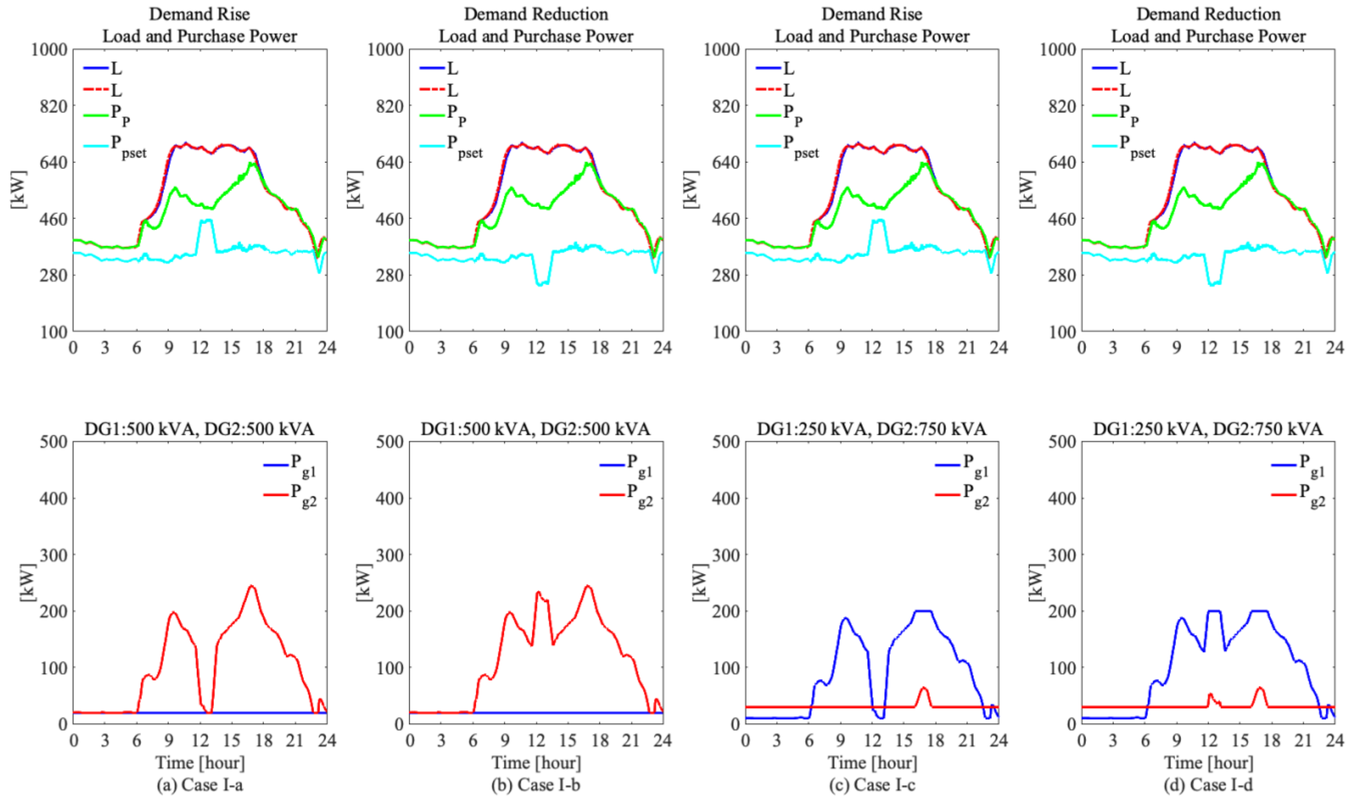

Fig. 9. Results for Case Study I.

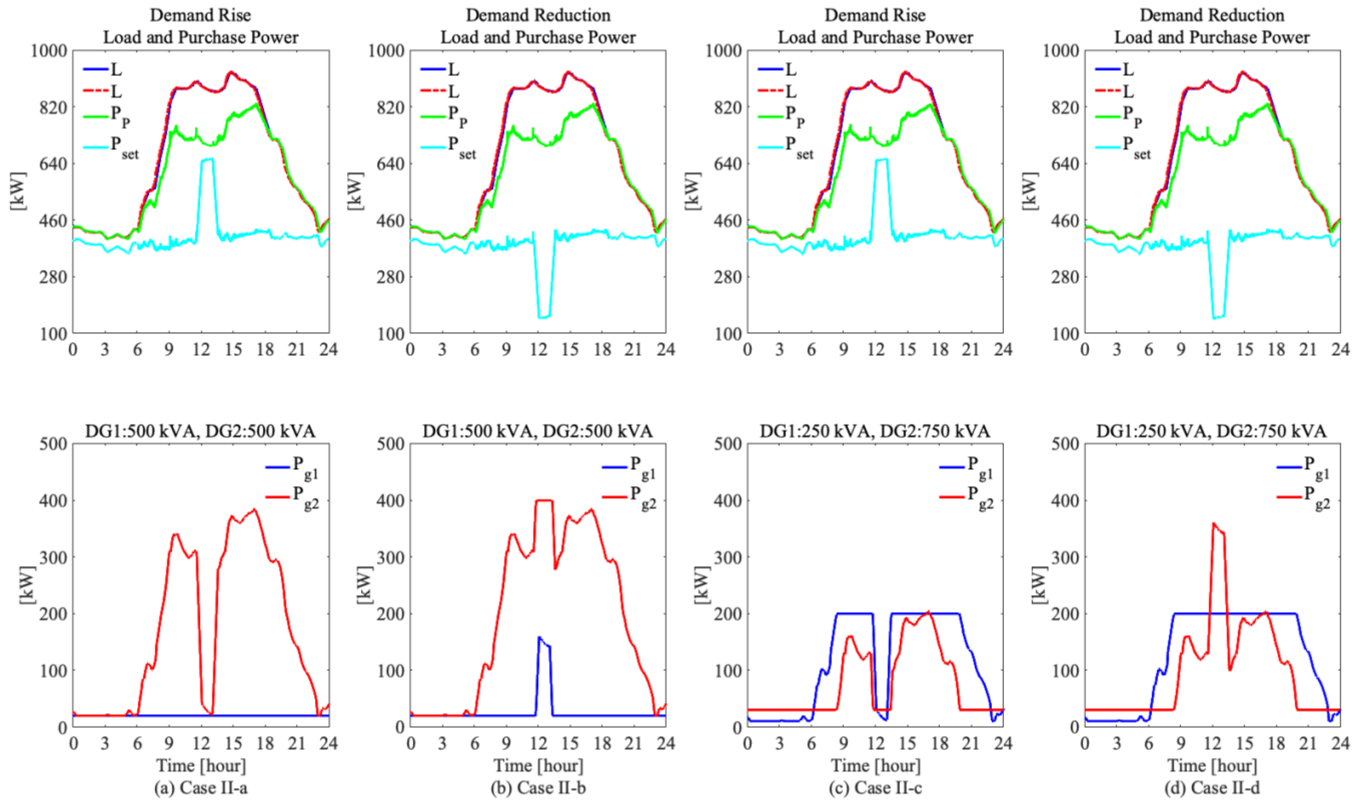

Fig. 10. Results for Case Study II.

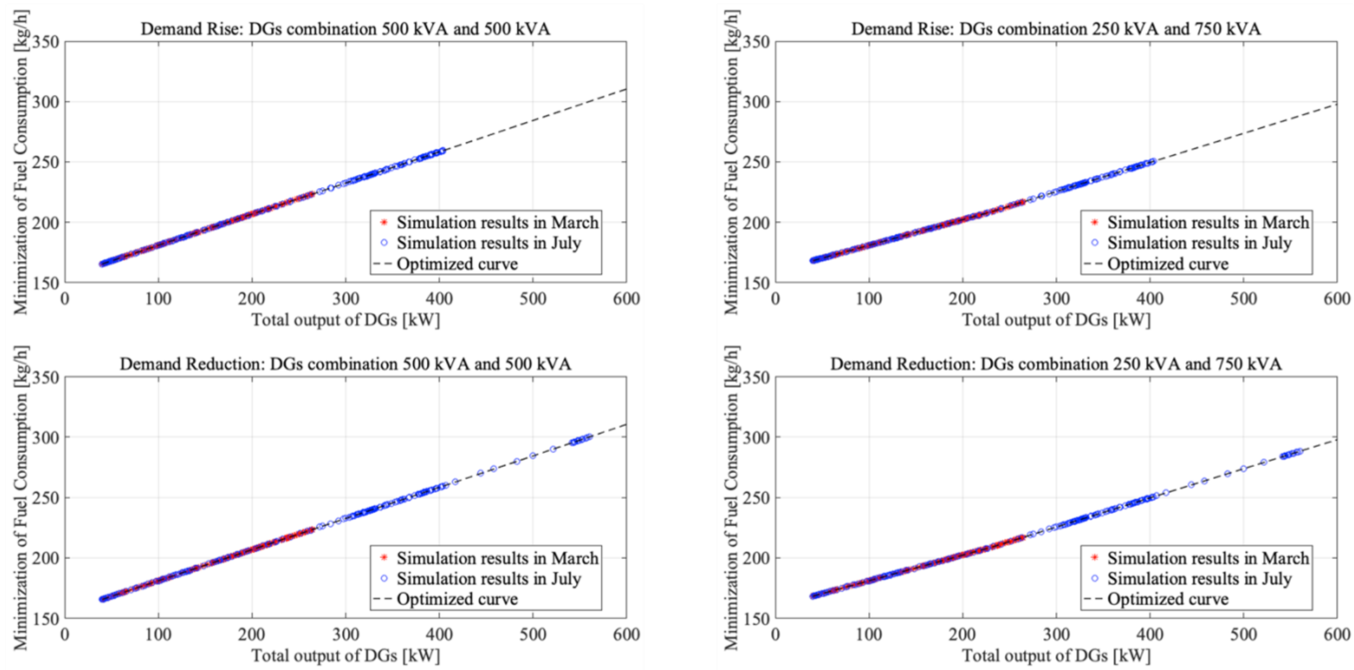

Fig. 11. Verification of optimized output for generators.

As a result, it shows that it can correspond a DR of ± 10 % in the season when the load is low at the hospital with contract demand 980 kW with 20 % of a PV. Furthermore, it is clarified that it can correspond to a DR of ± 25 % in the season when the load is high.

The proposed system for VPP that combination of DGs and PV, the DGs is responding to demand and does not suppress PV output, so the fuel consumption of the DGs can be minimized. The operation of the two DGs is optimized by the linear programing method to minimize fuel consumption.

Figure 11 shows the verification of optimized output for generators. The optimization curve as a design can be calculated minimization of fuel consumption against generator output using through Eq 6 and Eq 13, as shown in broken black line of Fig 11. The asterisk and circle marker represents the simulation results of overall generators output in Fig 9 and Fig 10, respectively. It is confirmed that fuel optimization is working effectively because the relationship between the generator output [kW] and the fuel consumption [kg/h] during operation is distributed on the optimization curve.

5. Conclusions and Outlook

This paper presents an operation method for diesel generators, which is applied to the demand side response as a virtual power plant with renewable energy for usage in a hospital. The proposed method can scale the measured PV output to the actual load at a disaster base hospital and provide it to the model.

The results are summarized as follows:

(1) A load prediction method that uses a machine learning with actual hospital data and weather information data recorded by the Japan Meteorological Agency is proposed using MATLAB.

(2) The machine learning used the weather information data and actual hospital load as the one-step-previous load, and the error in March is 2.0 kW to 2.8 kW when evaluated by RMSE. In July, there is an error of 2.2 kW to 3.6 kW. It is clarified that the error is within 0.37 % of contract power 980 kW at rated.

(3) The output of the predicted load is optimized by linear programming to minimize the fuel consumption, and an algorithm is established to allocate demand between two generators.

(4) It is clarified that a DR of 10 % in the season when the load is low and a DR of 25 % in the season when the load is high might correspond at the hospital with a contract demand of 980 kW and 20 % of a PV.

There is no fuel cost for power generation because DGs are operated with fuel that makes a plan to be discarded due to deterioration. Since all reward for DR from the operation of DGs is benefit, the reward can be compensated for the cost of purchasing new fuel for emergencies. An optimization and operation method of fuel tank capacity is a research task in future work.

Acknowledgements

We would like to thank Shimabara Hospital in Nagasaki Prefecture for providing their hospital load data. We were able to this research carried out by their cooperation.

This work was supported by JSPS KAKENHI Grant Number JP21K04559.

References

[1] “Damage from Typhoon Jebi,” White Paper Disaster Management in Japan, Director General for Disaster

Management Cabinet Office, Government of Japan, pp. 17-21, 2019.

[2] "About the damage situation to affect an earthquake to assume Kumamoto," Cabinet Office of Japan, 6th Jul. 2016.

[3] "Damage to the power supply infrastructure due to the Hokkaido Eastern Iburi Earthquake," White Paper Disaster Management in Japan, Director General for Disaster Management Cabinet, Government of Japan, pp. 22-33, 2019.

[4] "Disaster Management in Japan," Director General for Disaster Management Cabinet, Government of Japan, pp. 1-49, 2014.

[5] (IEIEJ/JSA) Japanese Industrial Standards (JIS) T1022, 2018.

[6] Allianz Risk Consulting (ARC), "Diesel Fuel Degradation," Tech Talk, Vol. 22, 2021.

[7] Y. Mizuno, Y. Tanaka, F. Kurokawa, and N. Matsui, "A New Approach of Optimum Energy Scheduling of Emergency Generators Using Linear Programing in a Large Hospital," in *Proc. 2016 International Conference on Renewable Energy Research and Application* (*ICRERA*), pp. 832-836, Nov. 2016.

[8] T. Baba, Y. Mizuno, Y. Tanaka, M. Tanaka, F. Kurokawa, I. Colak, and N. Matsui, "Comparison of Optimum Energy Schedule of Emergency Generators of Large Hospital with Renewable Energy System Using Mathematical Programing Method," in *Proc. 2017 International Conference on Renewable Energy Research and Application* (*ICRERA*), pp. 519-523, Nov. 2017.

[9] M. Tanaka, H. Eto, Y. Mizuno, N. Matsui, and F. Kurokawa, "GA based Optimization for Configuration and Operation of Emergency Generators in a Medical Facility Using Renewable Energy," *International Journal of Renewable Energy Research* (*IJRER*), Vol. 8, No. 1, pp. 200-207, 2018.

[10] Y. Mizuno, T. Baba, Y. Tanaka, M. Tanaka, F. Kurokawa, I. Colak, and N. Matsui, "A New Load Prediction Method and Management of Distributed Power System in Island Mode of a Large Hospital," in *Proc. 2018 International Conference on Renewable Energy Research and Application* (*ICRERA*), pp. 1215-1220, Nov. 2018.

[11] T. Baba, Y. Mizuno, Y. Tanaka, F. Kurokawa, and N. Matsui, "Evaluation of An Island Operation Method of Smart Hospital Grid Using A Power Emulation System," in *Proc. 2018 international conference on Smart Grid* (*icSmartGrid*), pp. 98-101, Dec. 2018.

[12] Y. Mizuno, Y. Tanaka, F. Kurokawa, and N. Matsui, "A Hospital Grid with Renewable Energy System Applied to Virtual Power Plant," in *Proc. 2020 international conference on Smart Grid* (*icSmartGrid*), pp. 203-207, June 2020.

[13] S. V. Cotto and W. Lee, "Microgrid Modular Design for Tribal Healthcare Facilities: Kayenta Health Center PV System Case Study," *IEEE Transactions on Industry Applications*, Vol. 53, No. 6, pp. 5121-5129, 2017.

[14] B. N. Silva, M. Khan, and K. Han, "Futuristic Sustainable Energy Management in Smart Environments: A Review of Peak Load Shaving and Demand Side Response Strategies, Challenges, and Opportunities," *Sustainability*, pp. 1-23, Dec. 2020.

[15] H. Yang, M. Li, Z. Jiang, and P. Zhang "Multi-Time Scale Optimal Scheduling of Regional Integrated Energy Systems Considering Integrated Demand Side Response," *IEEE Access*, pp. 5080-5090, Jan. 2020.

[16] Z. Jiang, Q. Ai, and R. Hao "Integrated Demand side response Mechanism for Industrial Energy System Based on Multi-Energy Interaction," *IEEE Access*, vol. 7, pp. 66336-66346, Jan. 2019.

[17] M. G. M. Abdolrasol, M. A. Hannan, A. Mohamed, U. A. U. Amiruldin, I. B. Z. Abidin, and M. N. Uddin, "An Optimal Scheduling Controller for Virtual Power Plant and Microgrid Integration Using the Binary Backtracking Search Algorithm," *IEEE Transactions on Industry Applications*, Vol. 54, No. 3, pp. 2834-2844, May/June. 2018.

[18] D. J. C. MacKay, "Bayesian Interpolation," *Neural Computation*, Vol. 4, No. 3, pp. 415-447, 1992.

[19] Q. Long, H. Yu, F. Xie, N. Lu, and D. Lubkeman, "Diesel Generator Model Parameterization for Microgrid Simulation Using Hybrid Box-Constrained Levenberg-Marquardt Algorithm," *IEEE Transactions on Smart Grid*, Vol. 12, No. 2, pp. 943-952, Sep. 2020.

[20] F. Y. Xu, X. Cun, M. Yan, H. Yuan, Y. Wang, and L. L. Lai, "Power Market Load Forecasting on Neural Network With Beneficial Correlated Regularization," *IEEE Transactions on Industrial Informatics*, Vol. 14, No. 11, pp. 5050-5059, Nov. 2018.

[21] K. Methaprayoon, W-J. Lee, S. Rasmiddatta, J. R. Liao, and R. J. Ross, "Multistage Artificial Neural Network Short-Term Load Forecasting Engine With Front-End Weather Forecast," *IEEE Transactions on Industry Applications*, Vol. 43, No. 6, Nov./Dec. 2007.

[22] T. W. S. Chow and C.T. Leung, "Neural Network Based Short-Term Load Forecasting Using Weather Compensation," *IEEE Transactions on Power Systems*, Vol. 11, No. 4, Nov., 1736-1742, 1996.

[23] R. Darshi, M. A. Bahreini, and S. A. Ebrahim, "Prediction of Short-Term Electricity Consumption by Artificial Neural Networks Levenberg-Marquardt Algorithm in Hormozgan Province, Iran," in *Proc. 2019 5th Iranian Conference on Signal Processing and Intelligent Systems (ICSPIS)*, pp. 1-4, Dec. 2019.

[24] Dantzig, G.B., A. Orden, and P. Wolfe. "Generalized Simplex Method for Minimizing a Linear Form Under Linear Inequality Restraints." Pacific Journal Math., Vol. 5, pp. 183-195, 1955.

[25] K. Hiromasa, Y. Takabayashi, K. Shiota, K. Tanomura, S. Osaki, Y. Onoue, and K. Shimomura, "A Study of Generation Control System in Consideration of Renewable Energy Source," *The Transactions of the Institute of Electrical Engineers of Japan* B, A Publication of Power and Energy Society, Vol. 137, No. 2, pp. 93-101, 2007.

[26] "Cabinet Decision Made on the FY 2019 Annual Report on Energy," Agency for Natural Resources and Energy, Jun. 2020. Available: https://www.enecho.meti.go.jp/en/

[27] D. Santhusitha and K. Karunasingha, "Root Mean Square Error or Mean Absolute Error? Use their ratio as well," *Information Sciences*, Vol. 585, pp. 609-629, Mar. 2022.

[28] N. Nguyen and J. Mitra, "An Investigation into the Role of Gas Turbines in Supporting Renewable Energy Integration," in *Proc. 2018 North American Power Symposium* (*NAPS*), pp. 1-6, Sep. 2018.